minerals

MDPI

Article

The Influence of REE β-Diketone Complexes on the Corrosion Behaviour of Mild Steel and 304 SS in 3.5% NaCl Solution

Olatunde J. Lawal [1], Johannes H. Potgieter [1,2,*], Caren Billing [3] and David J. Whitefield [1]

[1] School of Chemical and Metallurgical Engineering, University of the Witwatersrand, Private Bag X3, Johannesburg 2050, South Africa; 2213721@students.wits.ac.za (O.J.L.); david.whitefield@wits.ac.za (D.J.W.)
[2] Department of Natural Science, Faculty of Science and Engineering, Manchester Metropolitan University, Manchester M1 5GD, UK
[3] Molecular Sciences Institute, School of Chemistry, University of the Witwatersrand, Private Bag X3, Johannesburg 2050, South Africa; caren.billing@wits.ac.za
* Correspondence: herman.potgieter@wits.ac.za

Abstract: In the present investigation, four REE β-diketone complexes, namely cerium acetylacetone, cerium hexafluoroacetylacetone, lanthanum acetylacetone, and lanthanum hexafluoroacetylacetone, were investigated as potential corrosion inhibitors for mild steel and 304 stainless steel in 3.5% NaCl solution. The corrosion-inhibition effects of the REE β-diketone complexes were investigated using weight-loss measurements and potentiodynamic polarisation scans. Surface analyses using optical microscopy and scanning electron microscopy (SEM) were used to investigate the morphology of the mild steel and 304 stainless steel after the weight-loss and potentiodynamic tests in 3.5% NaCl solution containing 0.5% mass per volume (m/v) concentration of the tested inhibitor. Fourier transform infrared spectroscopy and Raman spectroscopy were further used to probe the type of corrosion product film that forms on the surface of the tested samples. The obtained results revealed that the four REE β-diketone complexes are very effective inhibitors against corrosion of mild steel and 304 stainless steel in a 3.5% NaCl in a temperature range of 20–60 °C.

Keywords: REE β-diketone complexes; corrosion inhibitors; potentiodynamic polarisation; Raman spectroscopy

Citation: Lawal, O.J.; Potgieter, J.H.; Billing, C.; Whitefield, D.J. The Influence of REE β-Diketone Complexes on the Corrosion Behaviour of Mild Steel and 304 SS in 3.5% NaCl Solution. *Minerals* **2022**, *12*, 416. https://doi.org/10.3390/min12040416

Academic Editor: Kenneth N. Han

Received: 4 March 2022
Accepted: 23 March 2022
Published: 29 March 2022

1. Introduction

Mild steel (MS) and austenitic stainless steel (304 SS) are two of the most reliable and durable metals that are widely used in various industrial applications. This is largely due to their corrosion resistance and good mechanical properties, as well as their reasonable cost [1–3]. However, when these steels are exposed to a corrosive environment that contains chloride ions, they degrade and undergo pitting corrosion [4]. Pitting corrosion is considered to be one of the most dangerous forms of corrosion, because it is difficult to predict and detect. This is because the pits formed on the alloys are usually small and narrow with relatively minimal overall metal loss. Therefore, it can result in catastrophic failure of infrastructure without prior notice. Inhibitors are often employed to address this challenge. However, most of these inhibitors are highly toxic, carcinogenic, and thus hazardous to humans and the environment [5,6]. For this reason, there is a restriction of the use of such inhibitors, and a concerted drive is underway to replace these corrosion inhibitors with ones having a less negative ecological impact on the environment [6,7]. Over the years, researchers have found that various rare earth element (REE) compounds have shown good inhibiting properties in both acidic and alkaline environments and compare favourably to chromate compounds. These REE inhibitors could thus be a possible replacement for chromates.

Somers et al. [8] investigated rare-earth (La, Ce, Nd, and Y) 3-(4-methyl benzoyl) propanoate compounds, $REE(mbp)_3$, as corrosion inhibitors for mild steel in a 0.01 M NaCl

solution. Detailed surface analysis using an optical microscope and a scanning electron microscope after immersion and electrochemical tests, revealed that the inhibitors greatly improve the corrosion resistance of mild steel in the NaCl solution. Analysis from FTIR and EDS showed the presence of a thin film containing inhibitor components on the surface of the tested steel specimens.

Fragoza-Mar et al. [9] studied the efficacy of 1,3-diketone malonates as corrosion inhibitors for mild steel in an aqueous 1.0 M hydrochloric acid solution. Their study indicated that the efficiency of the inhibitors was 75–96% for an inhibitor concentration of 100 mg/L. Their efficiency improved when the temperature was increased from 25 to 55 °C. It was also shown that the inhibition is mainly related to the tautomerism of the compounds at equilibrium.

Nam et al. [10] conducted an investigation using cerium hydroxycinnamate as a corrosion inhibitor for mild steel in 0.6 M NaCl solution. Polarization results indicated that it can effectively inhibit mild steel corrosion in NaCl solution. The results also indicated that the cerium hydroxycinnamate behaved as a mixed inhibitor. Analysis carried out using electrochemical impedance spectroscopy (EIS) revealed that cerium hydroxycinnamate produced a protective deposit on the steel surface when the inhibitor concentration was increased from 0.22 mM to 0.63 mM. Several other researchers have investigated different REE compounds, such as cerium nitrate, cerium sulphate, lanthanum nitrate, cerium diethyldithiocarbamate, cerium chloride, lanthanum chloride, using different metal alloys varying from aluminium to mild steel. Their reports have shown that the REE compounds are highly effective corrosion inhibitors that can replace and match the inhibiting properties of chromic compounds [10–18]. Available research has also proved that REE chloride and β-diketones, which are the two major components used in formulation of REE β-diketone complexes, are environmentally friendly with no reported cases of toxicity in humans or other adverse ecological effects [5]. Other researchers have also used different di-carbonyl compounds (β-diketones) on their own as corrosion inhibitors in corrosive acidic and alkaline environments, without incorporation of metals ions in the structure [19–22]. The inhibition mechanism and effect of REE β-diketones complexes have, however, received little attention to date. The only metal acetylacetone compounds investigated so far were those of the transition metals zinc (II), manganese (II), cobalt (II), and copper (II) in phosphoric acid. The results obtained from these electrochemical tests showed promising results in the application of corrosion reduction of mild steel using 0.01M of each transition metal complex at 25 °C [23]. Therefore, in this present study, cerium and lanthanum complexes with acetylacetone ($CH_3COCHCOCH_3$) and hexafluoroacetylacetone ($CF_3COCHCOCF_3$) were investigated as potential green corrosion inhibitors for mild steel and 304 stainless steel in a 3.5% chloride medium. The investigation was not only aimed at finding more environmentally friendly and acceptable corrosion inhibitors that can reduce the degradation of steels in a chloride containing solution, but also to identify what type of inhibitor they are.

2. Experimental Procedures

2.1. Test and Inhibitor Solutions

Analytical-grade sodium chloride, cerium and lanthanum acetylacetone, and hexafluoroacetylacetone were purchased from Sigma Aldrich (Pty) Ltd. (Johannesburg, South Africa). The test solutions were prepared by dissolving NaCl in distilled water to produce a 3.5% NaCl solution. Thereafter, 0.5% (m/v) inhibitor was dissolved in separate NaCl solutions. Cerium acetylacetone ($Ce(acac)_3$), cerium hexafluoroacetylacetone ($Ce(hfac)_3$), lanthanum acetylacetone ($La(acac)_3$), and lanthanum hexafluoroacetylacetone ($La(hfac)_3$) complexes were used without further purification. The structural formulae of the four REE β-diketone complexes are shown in Figure 1.

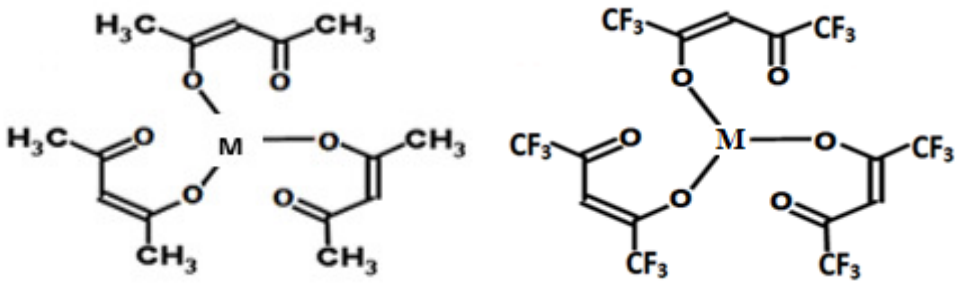

(**a**) (**b**)

Figure 1. Chemical structures of (**a**) metal acetylacetonate and (**b**) metal hexafluoroacetylacetone, where M = Ce or La, modified from [24].

2.2. Material Preparation

Mild steel and 304 SS specimens with a nominal composition (in wt.%), as shown in Table 1, were machined to a size of 2 cm × 3 cm × 0.95 cm and 2 cm × 3 cm × 0.12 cm, respectively, and ground with successively finer carbide papers ranging from 600 to 1500 grit size until a mirror-like surface was achieved. Thereafter, all surfaces were rinsed with distilled water and then with acetone to remove any possible oil and impurities from the surface and dried at room temperature. For the electrochemical corrosion tests, a mild-steel sample and 304 SS sample with a cross-sectional area of 0.7 cm^2 were prepared by mounting the sample in a resin to ensure that only the tested cross-sectional area of the samples were exposed to the NaCl solution. Thereafter, the samples were prepared in the same manner and procedure as those for the weight-loss experiments by grinding it to a mirror-like surface, using silicon carbide paper down to 2800 grit size and then using an alumina paste (6 microns) on a polishing cloth. The samples were then cleaned using distilled water, followed by drying with acetone before performing the electrochemical corrosion test.

Table 1. Nominal compositions of mild steel and 304 stainless steel.

Nominal Composition (wt.%)	C	S	Si	Mn	Cr	Ni	Mo	Fe
Mild steel	0.12	0.040	0.015	0.8	-	-		Balance
Stainless steel (type 304)	0.05	0.019	0.320	1.5	18.5	9.0	0.46	Balance

2.3. Weight-Loss Tests

Weight-loss tests were carried out after morphological analysis of the specimens. A hole of 3 mm diameter was drilled at one end of each sample, through which a chemically resistant polyethylene string was threaded to suspend the coupons in the corrosive media to avoid any galvanic corrosion. The polished samples were weighed (W_O), and then suspended in separate beakers containing the 3.5% NaCl solution doped with 0.5% wt. (m/v) REE β-diketone complex at room temperature. Control samples were also tested in 3.5% NaCl solutions without inhibitor. After 45 days of immersion, the coupons were cleaned with a nylon brush, rinsed with de-ionized water, and finally with acetone (obtained from Sigma Aldrich (Pty) Ltd., South Africa), and then air-dried and reweighed (W_1). Each set of experiments were performed in triplicate and the standard deviation for each was calculated. The average corrosion rate, (CR_{AV}), in micrometres per year (μmpy), and the inhibition efficiency (IE), were calculated using Equations (1) and (2), respectively.

$$\text{Corrosion rate (CR)} = 3.65 \times 10^6 \frac{W_O - W_1}{DAT} \quad (1)$$

where W_O and W_1 are the mass of the coupon before and after immersion (in grams),

D is the density of the coupon (in g/cm^3), T is the time of exposure (in days) and

A is the exposed area of the coupon in the test solution (in cm^2).

$$\text{The inhibitor efficiency IE, } (\%) = \frac{100(CR_{AV} - CR_{iAV})}{CR_{AV}} \quad (2)$$

where CR_{AV} and CR_{iAV} are the average corrosion rates of the uninhibited and inhibited steel samples, respectively.

2.4. Potentiodynamic Polarisation Experiments

The electrochemical polarisation experiments were performed using a Metrohm Autolab-1 Potentiostat/Galvanostat equipped with Nova 2.1 software (Utrecht, The Netherlands). The experiments were conducted at 20, 40, and 60 °C in a double jacketed corrosion cell containing 200 mL of NaCl solution. A three-electrode system with a platinum counter electrode and a Ag/AgCl (3M KCl) reference electrode was used and all potentials are quoted relative to this reference. Before commencing each experiment, the open circuit potential (OCP) was allowed to stabilize for 30 min. Thereafter, cathodic potentiodynamic polarisation scans employing a slow scan rate of 5 mV/s were initiated from 200 mV more negative than the OCP, followed by anodic polarisation scans up to 800 mV more positive than the OCP. Standard software was employed to obtain the corrosion parameters, such as corrosion potential (E_{corr}), Tafel slopes (βa and βc), and corrosion current density (i_{corr}), from the current density-potential graphs. The corrosion rate (CR), as well as inhibition efficiency (IE), were calculated using Equations (3)–(5).

$$CR = K\left(\frac{i_{corr}E_{EQ}}{D}\right) \quad (3)$$

CR is the rate of corrosion.

K is a constant whose value varies depending on the adopted units. For the density of a working electrode in g/cm^3 and a current density in $\mu A/cm^2$, the value of K will be taken as 3.27 micrometre/year (μm/y) [25].

i_{corr} is the corrosion current density (in $\mu A/cm^2$).

$$E_{EQ} = \left(\sum\left(\frac{f_{iZ_i}}{M_i}\right)\right)^{-1} \quad (4)$$

E_{EQ} = equivalent weight of mild steel and 304 stainless steel which were calculated to be 28.25 and 25.15, respectively.

$$IE = \frac{i_{corr} - i_{corr(inh)}}{i_{corr}} \times 100 \quad (5)$$

where i_{corr} and $i_{corr(inh)}$ are the corrosion current densities of the uninhibited and inhibited steel samples, respectively.

2.5. Surface Analysis of the Specimens

2.5.1. Scanning Electron Microscopy (SEM)

A JEOL (JSM 6390) Scanning Electron Microscope (SEM) equipped with energy disperse X-ray spectroscopy (EDX) was utilised. This instrument was used to check the surface morphology of the mild steel and 304 SS. EDX was used to qualitatively analyse the chemical composition of the film layer formed after exposure of the mild steel and stainless-steel electrodes exposed to a solution with and without inhibitors. This was undertaken after both the weight-loss tests and electrochemical tests in 3.5% NaCl solution.

2.5.2. Optical Microscopy

An Olympus GX 41F optical microscope, with a magnification up to 500×, was used to examine the surface microstructure of the specimens before and after immersion in the solutions with or without inhibitor for 45 days.

2.5.3. Raman Spectroscopy (RS)

Raman spectra were acquired using the 514.5 nm line of a Lexel Model 95 SHG argon-ion laser as an excitation source and a Horiba LabRAM HR Raman spectrometer equipped with a high-sensitivity Olympus BX41 microscope. Raman spectroscopy (RS) was used to map the surface of the steel specimens to analyse the nature of the adsorbed film formed on the surface during the corrosion experiments.

2.5.4. Fourier-Transform Infrared Spectroscopy (FTIR)

The infrared (IR) spectra were recorded at room temperature using a Perkin Elmer Fourier-transform-attenuated total reflectance—infrared spectrometer spectrum 2 (FT-ATR-IR-2) in the range from 4000-420 cm^{-1}.

3. Results and Discussion

3.1. Corrosion Measurements via Weight-Loss Tests

The inhibition of the corrosion of the mild steel and 304 SS after exposure to a solutions without and with 0.5% wt. (m/v) concentration of $Ce(acac)_3$, $Ce(hfac)_3$, $La(acac)_3$, and $La(hfac)_3$ inhibitors was examined at room temperature (approximately 25 °C) using weight-loss measurements. After 45 days of immersion in each inhibited solution, the average corrosion rates were calculated and are presented in Table 2. Whereas all four corrosion inhibitors were only effective to a degree in reducing the corrosion rate of mild steel in the 3.5% NaCl solution, they were 100% effective in stopping any corrosion of the stainless steel. There was not much difference in the degree of protection of the mild steel with a change in the metal ion in the complex of the inhibitor, or the β-diketone complex. A visual inspection of the coupons that were immersed in a solution containing $Ce(acac)_3$, $Ce(hfac)_3$, $La(acac)_3$, and $La(hfac)_3$ showed a brownish deposit, presumably a rare-earth oxide or hydroxide covering the surface of the coupon. The colour of the coupons remained intact after being washed with de-ionised water and rinsed with acetone. EDX analysis revealed that the colour of the coupons could have been due to a corrosion product film, which predominantly contained the rare-earth element compounds used as inhibitors. EDX spectra are shown in Figure 2. This observation had been reported by several authors using REE compounds, who all concluded that the observed colour on the surface of the investigated specimens in the presence of REE compounds was a result of the formation of a rare earth oxide on the surface of the coupons [26–31].

Table 2. Comparison of corrosion rate of mild steel and 304 SS and inhibition efficiency in the absence and presence of $Ce(acac)_3$, $Ce(hfac)_3$, $La(acac)_3$, and $La(hfac)_3$ inhibitors in 3.5% NaCl solution.

	REE Inhibitor	CR with Inhibitor (μm/y)	CR without Inhibitor (μm/y)	IE (%)
Mild steel	$Ce(acac)_3$	42	156	74
	$Ce(hfac)_3$	41	166	75
	$La(acac)_3$	43	180	76
	$La(hfac)_3$	45	159	72
304 SS	$Ce(acac)_3$	0.0	0.7498	100
	$Ce(hfac)_3$	0.0	0.6722	100
	$La(acac)_3$	0.0	0.5430	100
	$La(hfac)_3$	0.0	0.6378	100

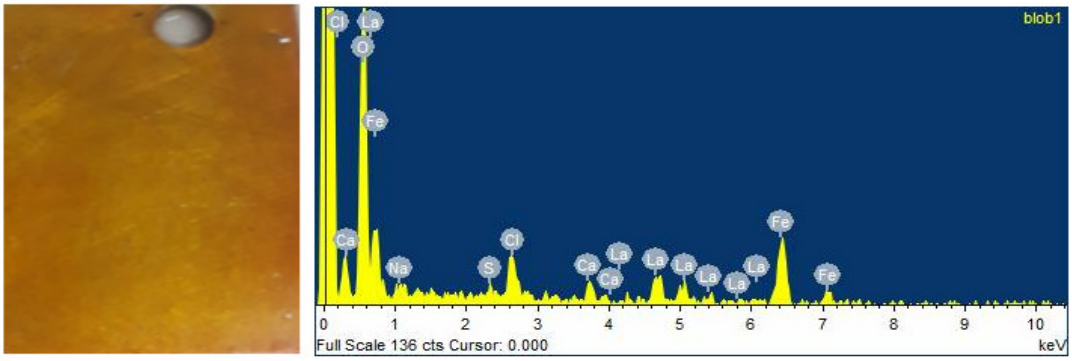

(**a**)

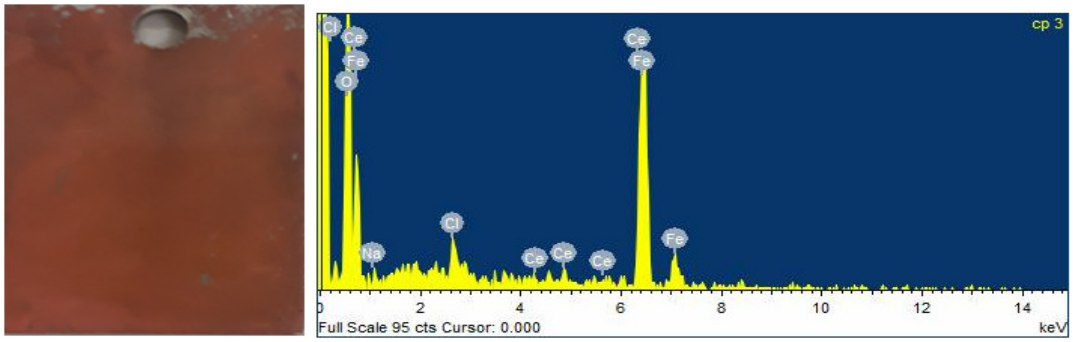

(**b**)

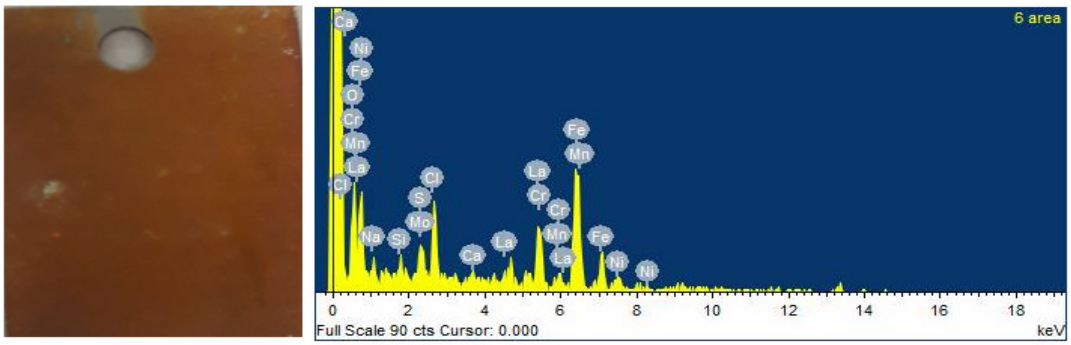

(**c**)

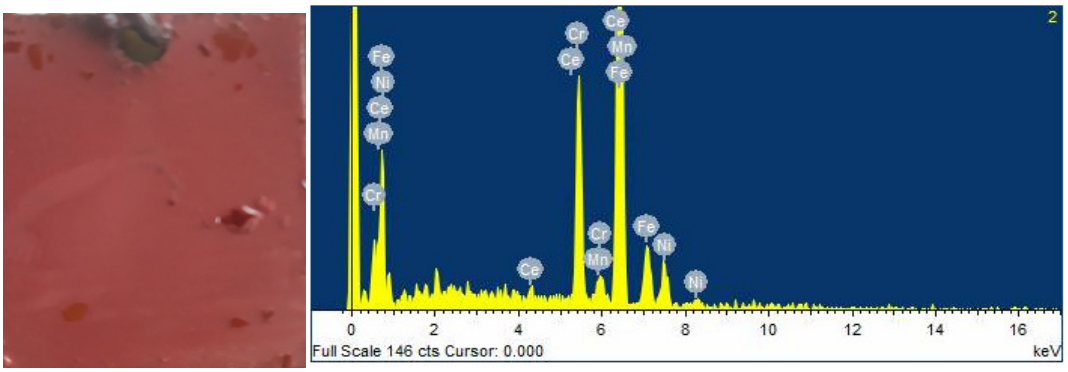

(**d**)

Figure 2. EDX spectra of (**a**) and (**b**) MS coupon exposed to 3.5% NaCl solution containing $La(acac)_3$ and $Ce(acac)_3$, (**c**,**d**) 304 SS inhibited with $La(hfac)_3$ and $Ce(hfac)_3$.

3.2. Potentiodynamic Polarisation Measurements

The electrochemical parameters obtained from the potentiodynamic polarisation (PDP) curves for MS and 304 SS in 3.5% NaCl solution with and without inhibitors at 20, 40 and 60 °C are tabulated in Tables 3 and 4. The data obtained from the PDP curves showed that the corrosion rate values decreased slightly in the presence of REE β-diketone inhibitor compared to a 3.5% NaCl solution without inhibitor. This phenomenon can be attributed to the adsorption of REE β-diketone inhibitor onto the metal surface, as suggested by other authors [32,33]. There was remarkably little change in and difference between the corrosion potential and corrosion current density of the mild steel in the 3.5% NaCl solution with any one of the four corrosion inhibitors investigated, compared to the mild steel under the same conditions when no inhibitor was used at all. This was in agreement with the low corrosion inhibitor efficiency calculated for all four corrosion inhibitors evaluated. It was clear that a concentration of 0.5% was insufficient to provide corrosion protection for mild steel in 3.5% NaCl at all the tested temperatures. The general trend was for the cathodic Tafel constants to decrease compared to the cases where no inhibitor was present. Furthermore, when the $La(hfac)_3$ inhibitor was used, the corrosion potential was distinctly more negative compared to the samples exposed in the sodium chloride solution without any inhibitor. Both these indications point to the REE β-diketone inhibitors, or at the very least the $La(hfac)_3$ inhibitor, acting as a cathodic corrosion inhibitor.

Table 3. Electrochemical parametersof MS obtained from the potentiodynamic polarisation curves.

3.5% NaCl solution without inhibitor						
Temp. (°C)	E_{corr} (V)	i_{corr} (A/cm^2)	βa (mV/dec)	βc (mV/dec)	CR (μm/y)	IE (%)
20	−0.552	1.62×10^{-5}	54	360	191	
40	−0.626	2.41×10^{-5}	42	314	284	
60	−0.591	2.89×10^{-5}	64	284	340	
			$Ce(acac)_3$			
Temp. (°C)	E_{corr} (V)	i_{corr} (A/cm^2)	βa (mV/dec)	βc (mV/dec)	CR (μm/y)	IE (%)
20	−0.434	1.01×10^{-5}	109	186	118	38.0
40	−0.604	1.54×10^{-5}	69	207	181	36.0
60	−0.630	1.60×10^{-5}	47	215	188	33.5
			$Ce(hfac)_3$			
Temp. (°C)	E_{corr} (V)	i_{corr} (A/cm^2)	βa (mV/dec)	βc (mV/dec)	CR (μm/y)	IE (%)
20	−0.554	1.00×10^{-5}	135	81	104	46.0
40	−0.643	1.57×10^{-5}	54	120	163	43.0
60	−0.597	1.94×10^{-5}	46	301	200	41.0
			$La(acac)_3$			
Temp. (°C)	E_{corr} (V)	i_{corr} (A/cm^2)	βa (mV/dec)	βc (mV/dec)	CR (μm/y)	IE (%)
20	−0.575	1.04×10^{-5}	126	211	109	36.0
40	−0.592	1.61×10^{-5}	125	182	169	33.0
60	−0.584	2.09×10^{-5}	66	151	219	28.0
			$La(hfac)_3$			
Temp. (°C)	E_{corr} (V)	i_{corr} (A/cm^2)	βa (mV/dec)	βc (mV/dec)	CR (μm/y)	IE (%)
20	−0.650	1.01×10^{-5}	212	116	119	38.0
40	−0.637	1.58×10^{-5}	69	164	186	34.0
60	−0.691	2.04×10^{-5}	92	127	240	29.0

Table 4. Electrochemical parameters of 304 SS obtained from the potentiodynamic polarization curves.

3.5% NaCl solution without inhibitor						
Temp. (°C)	E_{corr} (V)	i_{corr} (A/cm^2)	βa (mV/dec)	βc (mV/dec)	CR (μm/y)	IE (%)
20	−0.287	3.66×10^{-7}	351	67	3.79	
40	−0.359	1.40×10^{-6}	76	49	14.50	
60	−0.370	4.47×10^{-6}	123	57	56.66	
			$Ce(acac)_3$			
Temp.(°C)	E_{corr} (V)	i_{corr} (A/cm^2)	βa (mV/dec)	βc (mV/dec)	CR (μm/y)	IE (%)
20	−0.134	5.84×10^{-8}	243	79	0.60	84
40	−0.157	3.5×10^{-7}	206	86	3.63	75
60	−0.190	2.14×10^{-6}	391	100	22.17	52
			$Ce(hfac)_3$			
Temp. (°C)	E_{corr} (V)	i_{corr} (A/cm^2)	βa (mV/dec)	βc (mV/dec)	CR (μm/y)	IE (%)
20	−0.122	4.07×10^{-8}	482	70	0.42	89
40	−0.132	3.73×10^{-7}	345	93	3.49	76
60	−0.135	2.11×10^{-6}	323	102	11.50	53
			$La(acac)_3$			
Temp. (°C)	E_{corr} (V)	i_{corr} (A/cm^2)	βa (mV/dec)	βc (mV/dec)	CR (μm/y)	IE (%)
20	−0.243	1.02×10^{-7}	379	72	1.07	72
40	−0.198	1.01×10^{-6}	344	77	10.46	25
60	−0.177	3.53×10^{-6}	185	80	36.56	21
			$La(hfac)_3$			
Temp. (°C)	E_{corr} (V)	i_{corr} (A/cm^2)	βa (mV/dec)	βc (mV/dec)	CR (μm/y)	IE (%)
20	−0.126	8.13×10^{-8}	301	78	0.84	78
40	−0.156	3.85×10^{-7}	369	105	3.99	73
60	−0.162	2.05×10^{-6}	306	164	21.23	54

The potentiodynamic curves of the mild steel for all the tested temperatures and corrosion inhibitors in the 3.5% NaCl solutions are shown in Figure 3, while the corresponding test results with 304 SS under similar conditions are displayed in Figure 4.

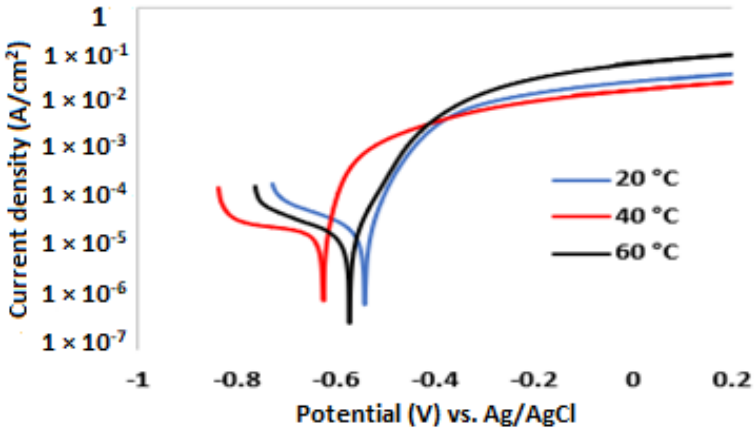

(**a**)

Figure 3. *Cont.*

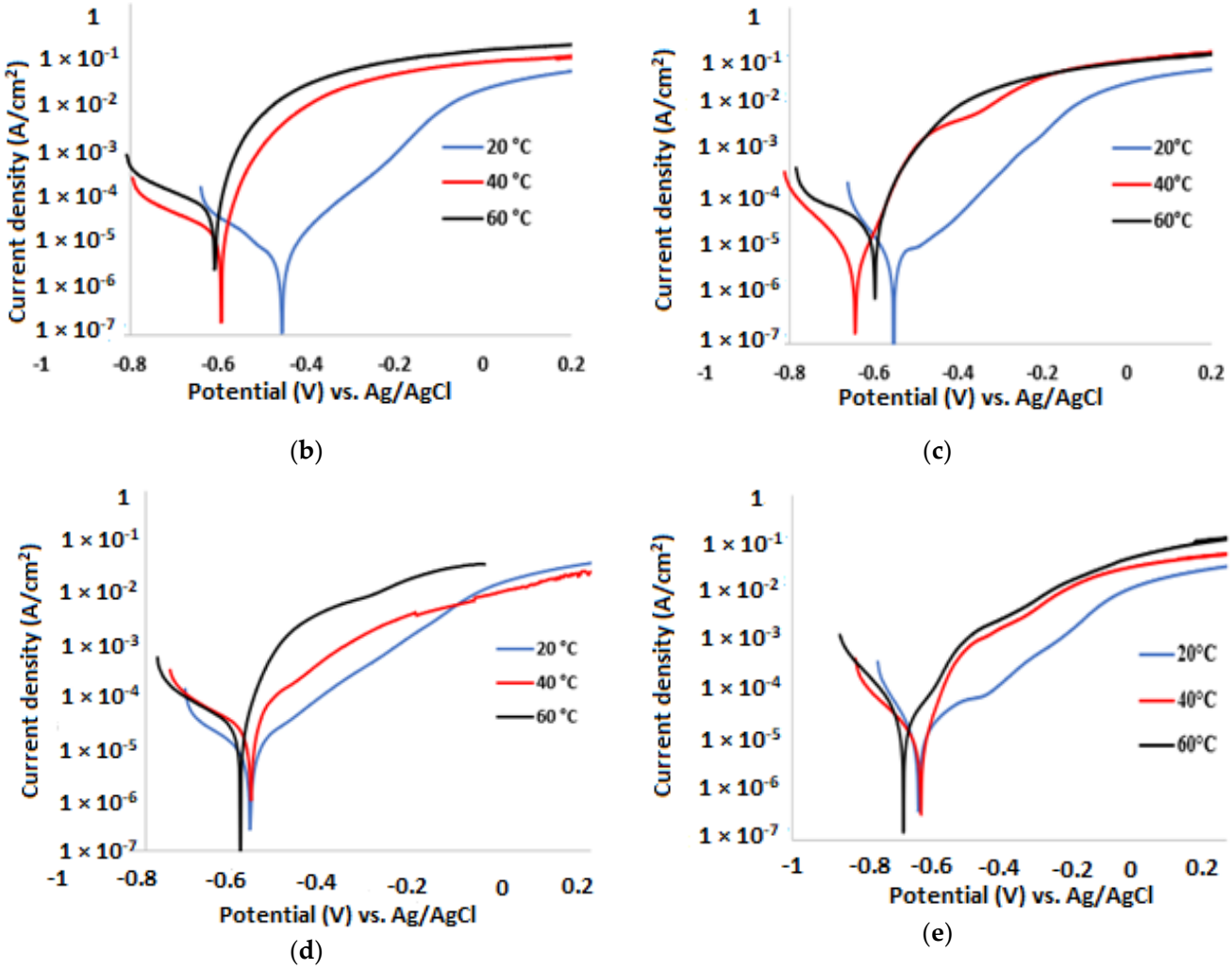

Figure 3. Potentiodynamic polarisation curves of mild steel in 3.5% NaCl solution with (**a**) MS without inhibitor, (**b**) $Ce(acac)_3$, (**c**) $Ce(hfac)_3$, (**d**) $La(acac)_3$, and (**e**) $La(hfac)_3$ inhibitor.

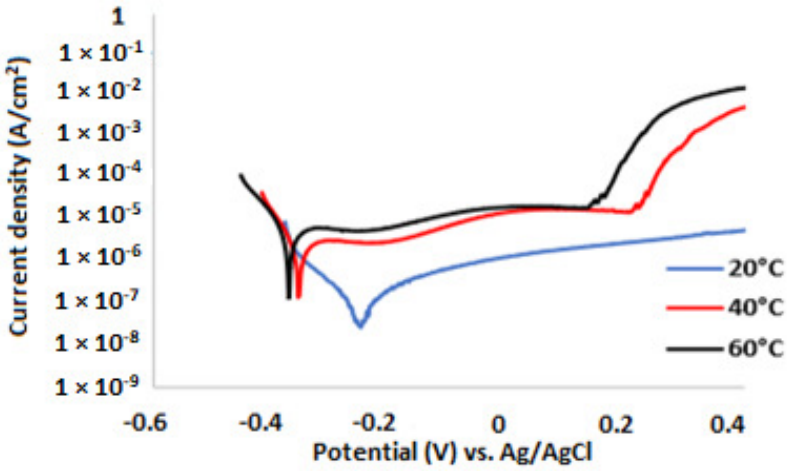

Figure 4. *Cont.*

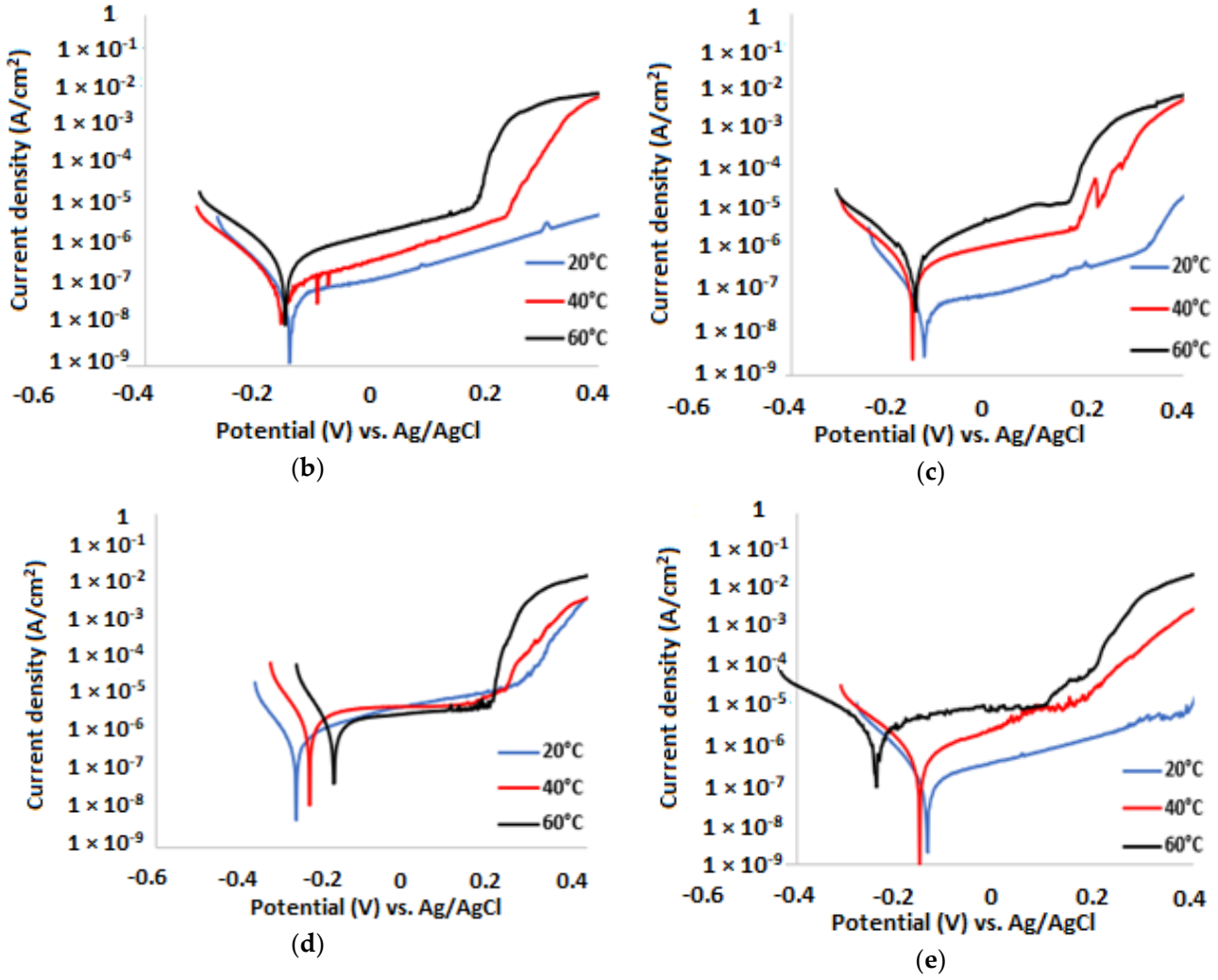

Figure 4. Potentiodynamic polarisation curves of 304 SS in 3.5% NaCl solution with (**a**) 304 SS without inhibitor, (**b**) $Ce(acac)_3$, (**c**) $Ce(hfac)_3$, (**d**) $La(acac)_3$, and (**e**) $La(hfac)_3$ inhibitor.

Table 4 summarises the relevant electrochemical parameters derived from the potentiodynamic curves in Figure 4 for the evaluations performed with 304 SS in the various solutions.

Two substantial deductions immediately became apparent when evaluating the results shown in Table 4. Firstly, there was generally a significant decrease in the corrosion rate of the material when the different corrosion inhibitors were present in the solution as compared to that in the solution without any inhibitor. With the stainless-steel samples exposed to 3.5% NaCl, there was a definitive shift in the corrosion potential to more noble values in the presence of all four corrosion inhibitors, hinting that they act as anodic-type inhibitors. The efficiency of the different inhibitors to reduce the corrosion rates in the NaCl solution with the stainless-steel samples was also substantially higher than in the case of the mild steel, especially at the lower temperatures. As was the case with the mild steel in the NaCl solution, these tests showed that the inhibitors were not 100% effective in their corrosion-inhibition efficiency. Secondly, there was a definite decrease in corrosion inhibitor efficiency with the increasing of the temperature of the corrosive solution, a trend that was not so clear or pronounced in the case of the mild steel samples when the solution temperature increased to 60 °C.

4. Surface Analyses of the Specimen

4.1. Optical Microscopy

The MS and 304 SS specimens before exposure and after the electrochemical tests in a NaCl solution and with $Ce(acac)_3$, $Ce(hfac)_3$, $La(acac)_3$, and $La(hfac)_3$ inhibitors showed some degree of surface pitting and general corrosion. The formation of pits was visible and they were uniformly distributed on the surface of the MS electrodes that were retrieved from NaCl solutions at 40 and 60 °C. However, with an added concentration of 0.5 wt.% (*m*/*v*) in $Ce(acac)_3$ or $La(acac)_3$ inhibitor, there was a reduction in the pitting corrosion of the mild steel, while no pitting was observed for 304 SS with $Ce(hfac)_3$ or $La(hfac)_3$ inhibitor. Micrographs after the potentiodynamic tests showed that both MS and 304 SS were well protected against localised corrosion. The observed results agree with the investigation of Somers et al. [8] and Forsyth et al. [34], where they used different REE compounds on mild steel and an aluminium alloy to prevent pitting corrosion. Boudellioua et al. [35] also confirmed this observation in their investigation when using cerium nitrate at an optimal concentration of 600 mg/L on mild steel in 0.1 M NaCl solution in a temperature range of 25–75 °C to reduce pitting corrosion.

The degree of pitting increased with an increase in temperature and the pits on the stainless-steel surface were far fewer and much smaller than those on the mild steel under similar conditions. The manner in which the appearance of the mild steel and stainless steel changed in the presence of the various corrosion inhibitors is illustrated in Figures 5 and 6.

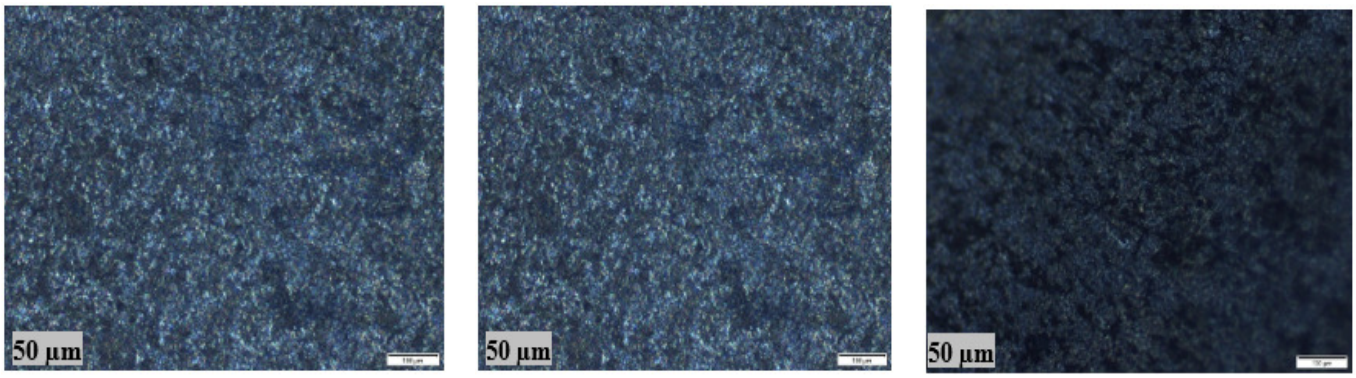

(**a**) (**b**) (**c**)

Figure 5. Optical micrographs of inhibited mild steel in 3.5% NaCl solution doped with $La(acac)_3$ at (**a**) 20 °C, (**b**) 40 °C, and (**c**) 60 °C.

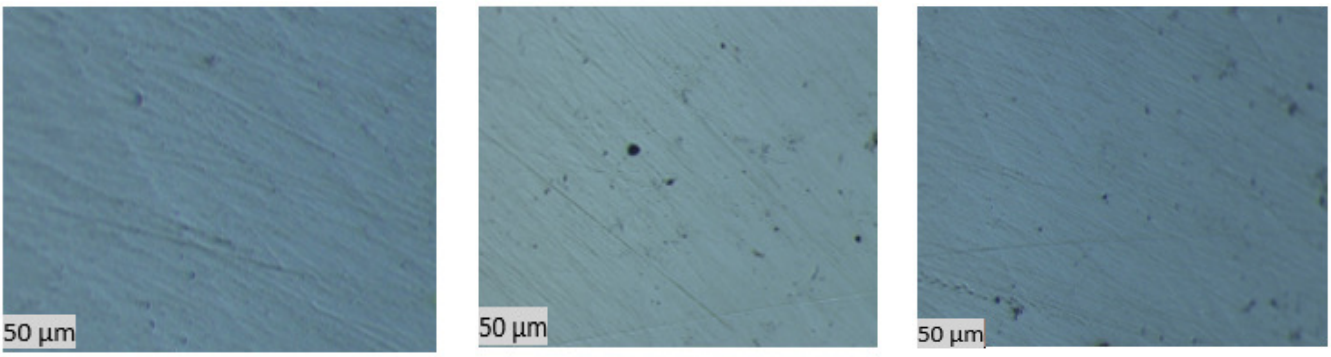

(**a**) (**b**) (**c**)

Figure 6. Optical micrographs of inhibited 304 SS in 3.5% NaCl solution doped with $Ce(hfac)_3$ at (**a**) 20 °C, (**b**) 40 °C, and (**c**) 60 °C.

From the micrographs displayed in Figures 5 and 6, it appears that there were fewer and smaller pits on the surfaces of the mild steel samples exposed to the sodium chloride solution when the inhibitors were present than without them. One could not really distinguish a difference between the pitting corrosion occurring in the presence of the two different inhibitors. It was therefore questionable if the type of REE in the inhibitor played a significant role in the efficiency of the inhibitor. This corresponded to the values summarised in Tables 3 and 4 in terms of the percentage efficiency of the different corrosion inhibitors. Further work with similar β-diketone inhibitors in other REE complexes can confirm whether this is indeed the case and should be pursued in future. Apart from the fact that there was clearly much less pitting on the surfaces of the stainless-steel samples compared to the mild-steel samples, similar observations could be made about the presence of the different corrosion inhibitors.

4.2. Scanning Electron Microscopy and Energy-Dispersive X-ray Spectroscopy Analysis (SEM/EDS)

Figures 7–10 show the SEM images of MS and 304 SS working electrodes before and after exposure with and without the REE β-diketone inhibitor complexes at 20 °C, 40 °C, and 60 °C. As the temperature of the solution containing $Ce(acac)_3$, $Ce(hfac)_3$, $La(acac)_3$, and $La(hfac)_3$ inhibitors increased to 60 °C, the surface morphologies of both MS and 304 SS changed compared to the ones retrieved at lower temperatures under the same conditions and similar environments. Analysis with EDS (Figure 11) on the MS and 304 SS electrode surfaces that were exposed to solutions that contained $Ce(acac)_3$, $Ce(hfac)_3$, $La(acac)_3$, and $La(hfac)_3$ revealed the formation of RE oxide and iron oxide containing films. These indicated that the main elements present in the corrosion product films were Ce or La, and Fe and O on the surfaces of MS and 304 SS electrodes. The observed results are in agreement with other authors' observations based on the use of REE compounds as corrosion inhibitors for different alloys [8,11,36].

Amadeh et al. [37] used a mixture of RE oxide (Ce and La) as a corrosion inhibitor for carbon steel in 0.6 M NaCl solutions. SEM and EDS analysis of the nature of the deposit formed on the surface of the tested sample revealed that the sample was covered with a layer of corrosion products consisting of particles with irregular shapes containing cerium (Ce) and iron (Fe) deposits.

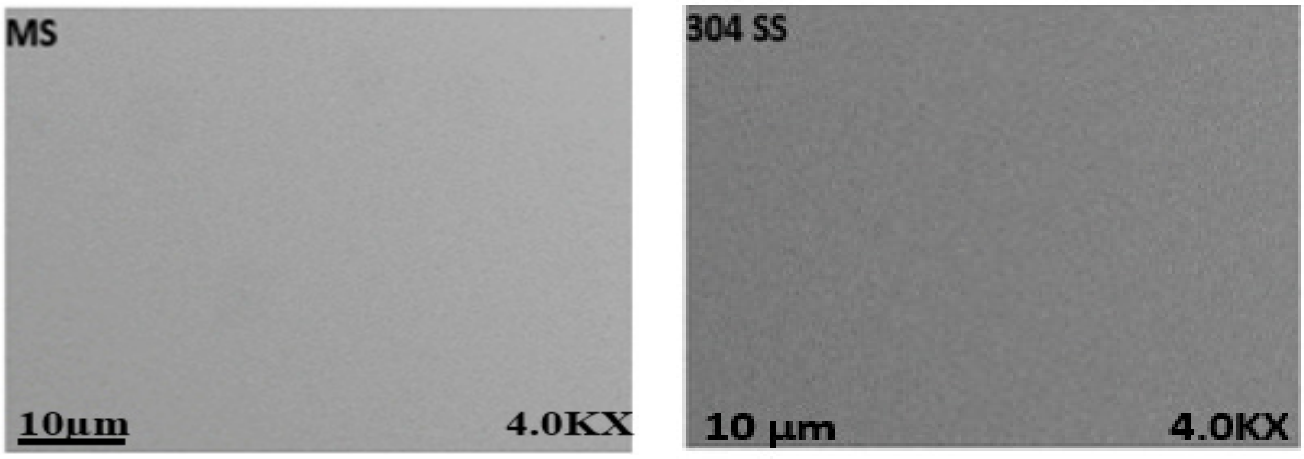

(**a**) (**b**)

Figure 7. SEM micrographs of (**a**) MS and (**b**) 304 SS electrode surfaces before exposure in NaCl solution.

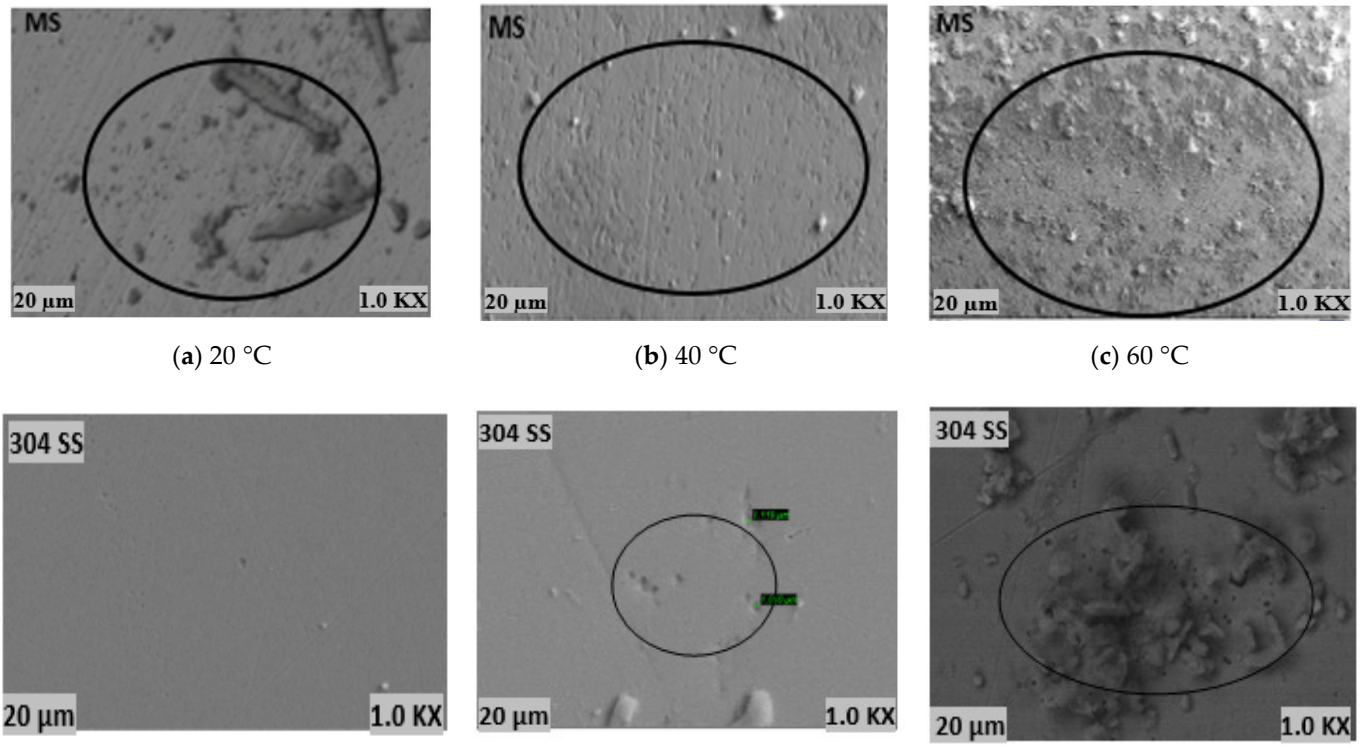

(**a**) 20 °C (**b**) 40 °C (**c**) 60 °C

(**d**) 20 °C (**e**) 40 °C (**f**) 60 °C

Figure 8. SEM micrographs of uninhibited (**a**–**c**) MS and (**d**–**f**) 304 SS sample surfaces obtained after exposure to 3.5% NaCl solution at 20 °C, 40 °C, and 60 °C.

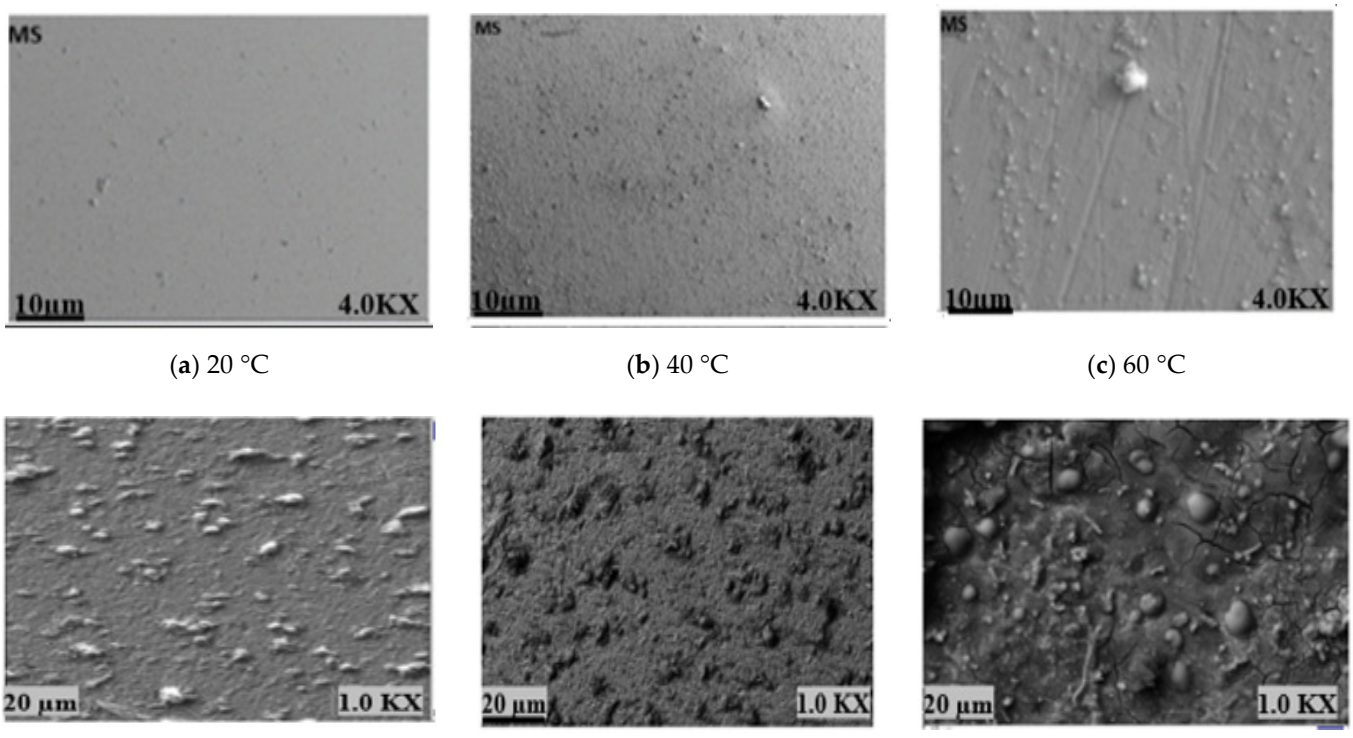

(**a**) 20 °C (**b**) 40 °C (**c**) 60 °C

(**d**) 20 °C (**e**) 40 °C (**f**) 60 °C

Figure 9. SEM micrographs of inhibited mild steel sample surfaces with (**a**–**c**) $Ce(acac)_3$ and (**d**–**f**) $La(acac)_3$ obtained after exposure to 3.5% NaCl solutions at 20 °C, 40 °C, and 60 °C.

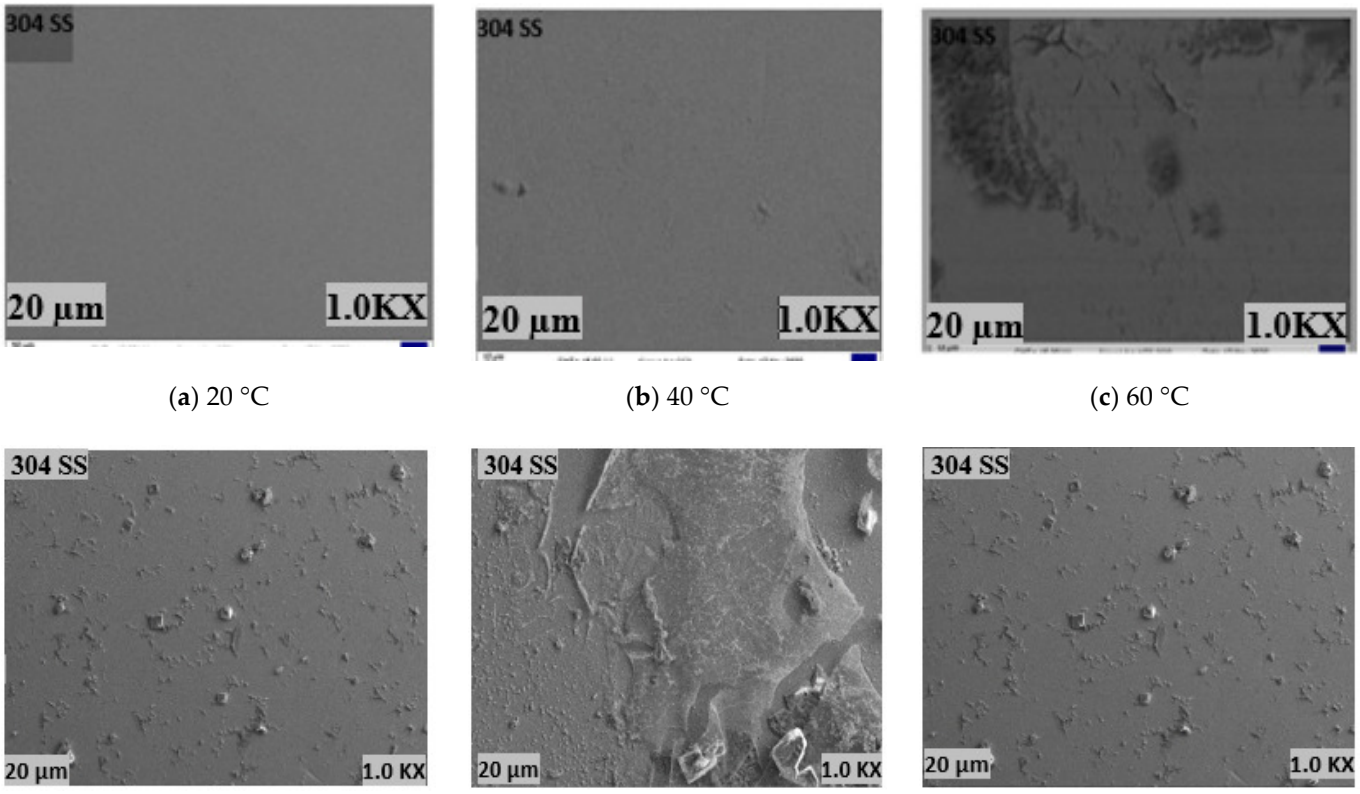

(**a**) 20 °C (**b**) 40 °C (**c**) 60 °C

(**d**) 20 °C (**e**) 40 °C (**f**) 60 °C

Figure 10. SEM micrographs of 304 SS sample surfaces inhibited with $Ce(hfac)_3$ (**a–c**) and $La(hfac)_3$ (**d–f**) obtained after exposure to 3.5% NaCl solutions at 20 °C, 40 °C, and 60 °C.

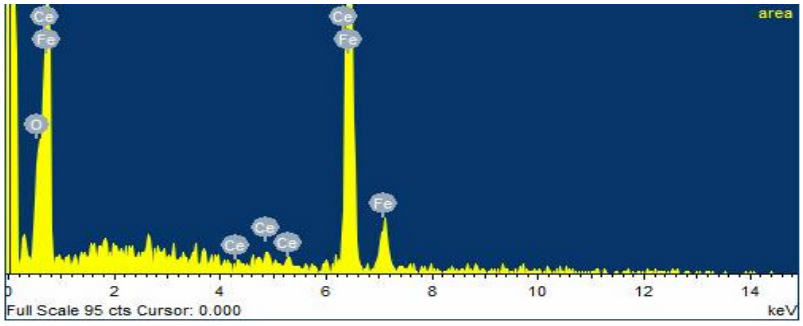

Element	Weight %	Atomic %
O K	5.52	17.13
Fe K	92.35	82.11
Ce L	2.13	0.76
Totals	100.00	

(**a**)

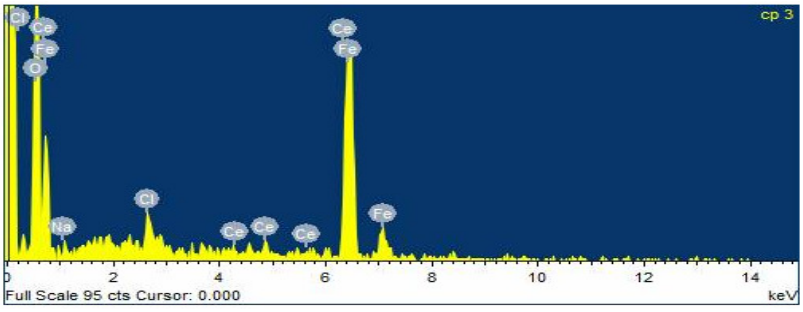

Element	Weight %	Atomic %
O K	29.97	59.88
Na K	0.54	0.75
Cl K	2.02	1.82
Fe K	64.37	36.84
Ce L	3.09	0.71
Totals	100.00	

(**b**)

Figure 11. *Cont.*

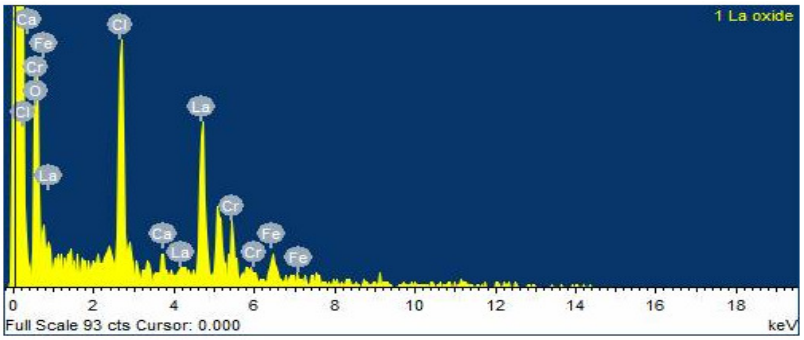

Element	Weight %	Atomic %
O K	22.69	58.65
Cl K	14.80	17.27
Ca K	1.26	1.30
Cr K	3.14	2.49
Fe K	6.76	5.00
La L	51.36	15.29
Totals	100.00	

(**c**)

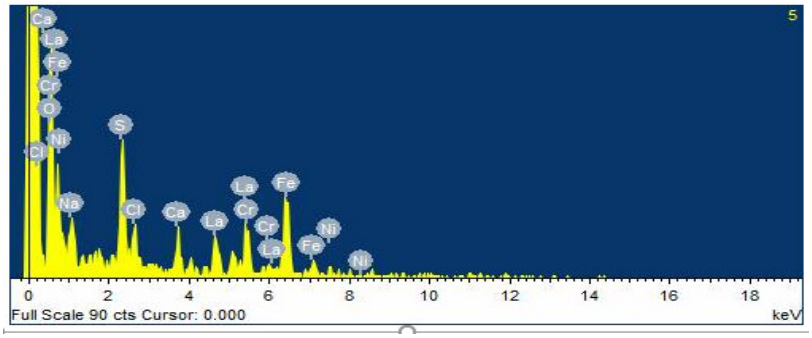

Element	Weight %	Atomic %
O K	27.36	54.65
Na K	4.84	6.73
S K	8.02	7.99
Cl K	2.78	2.50
Ca K	3.40	2.71
Cr K	8.62	3.30
Fe K	25.99	14.87
Ni K	2.77	1.51
La L	16.23	3.73
Totals	100.00	

(**d**)

Figure 11. EDS of (**a**,**b**) MS in 3.5% NaCl solution containing 0.5% wt. (*m*/*v*) of $Ce(acac)_3$ and $Ce(hfac)_3$ and (**c**,**d**) 304 SS with $La(acac)_3$ and $La(hfac)_3$.

A similar investigation was carried out by Somers et al. [8] using SEM/EDS analysis on the film deposits formed on mild steel when rare-earth (La, Ce. Nd, and Y) methyl benzoyl propanoate compounds, $REE(mbp)_3$, were used as corrosion inhibitors in 0.01 M NaCl solution. EDS analysis showed that the corrosion product deposits predominantly consisted of compounds containing La and Y together with a large amount of Fe and O. For Ce and Nd methyl benzoyl propanoate complexes, only Fe and O were detected with no indication of Ce and Nd elements as part of the corrosion product which had been formed on the surface on the mild steel.

Mohammadi et al. [18] studied corrosion-inhibitive pigment for aluminium AA2024-T3 by using a cerium diethyldithiocarbamate complex (Ce-DEDTC). The SEM/EDS results of the tested alloy indicated that the surface of the specimen from the solution containing Ce-DEDTC contained C, N, S, and Ce elements in the inhibitor film on the aluminium surface.

4.3. Surface Mapping of the Mild Steel and 304 Stainless Steel

4.3.1. Fourier Transform Infrared Spectroscopy Analysis

To understand the inhibition mechanism, FTIR analysis was carried out to probe the surfaces of the mild steel and 304 SS samples that were immersed in solutions containing $Ce(acac)_3$, $La(acac)_3$, $Ce(hfac)_3$, or $La(hfac)_3$ after the electrochemical tests. The ν(OH) bands observed above 3000 cm^{-1} for the REE complexes were shifted to the 2967–2874 cm^{-1} range on the surface of the steel. The frequency bands observed at 1408–1632 cm^{-1} on the surface of the examined steel could be assigned to C=O. The disappearance and shift in the frequencies as observed in the spectra suggested that adsorption of the film on the surface of the investigated steel samples had taken place [38]. While the O–H band shift was significant for all four the corrosion inhibitors between the complex in its pure form and the complex present in the corrosion products, it was not always the case with the shift in the C=O bands. Only the C=O bands of the La type inhibitors displayed a substantial

shift in their position in the corrosion film products compared to the pure compounds. This was the first indication from all the collected results that the metal in the β-diketone can indeed play a role in the inhibitor's performance. The C-H in-plane and out of plane frequency bands were also observed, but these bands did not take part in the film formation as there were no significant changes observed in the band. For comparison, the frequency of the absorption band of the REE complexes and the corrosion products as well as the IR spectra are presented in detail in Table 5 and Figure 12.

Table 5. IR frequency bands of REE(β-diketone)$_3$ inhibitors and the corrosion products formed on mild steel and 304 stainless steel.

Inhibitor Used	Inhibitor Only		Corrosion Product	
	Frequency (cm^{-1})	Assignment	Frequency (cm^{-1})	Assignment
Ce(acac)$_3$	1584 3134	C=O O-H	1576 2967	C=O OH
La(acac)$_3$	1595 3335	C=O O-H	1408 2967	C=O OH
Ce(hfac)$_3$	1644 3041	C=O O-H	1632 2921	C=O OH
La(hfac)$_3$	1648 3041	C=O O-H	1615 2920	C=O OH

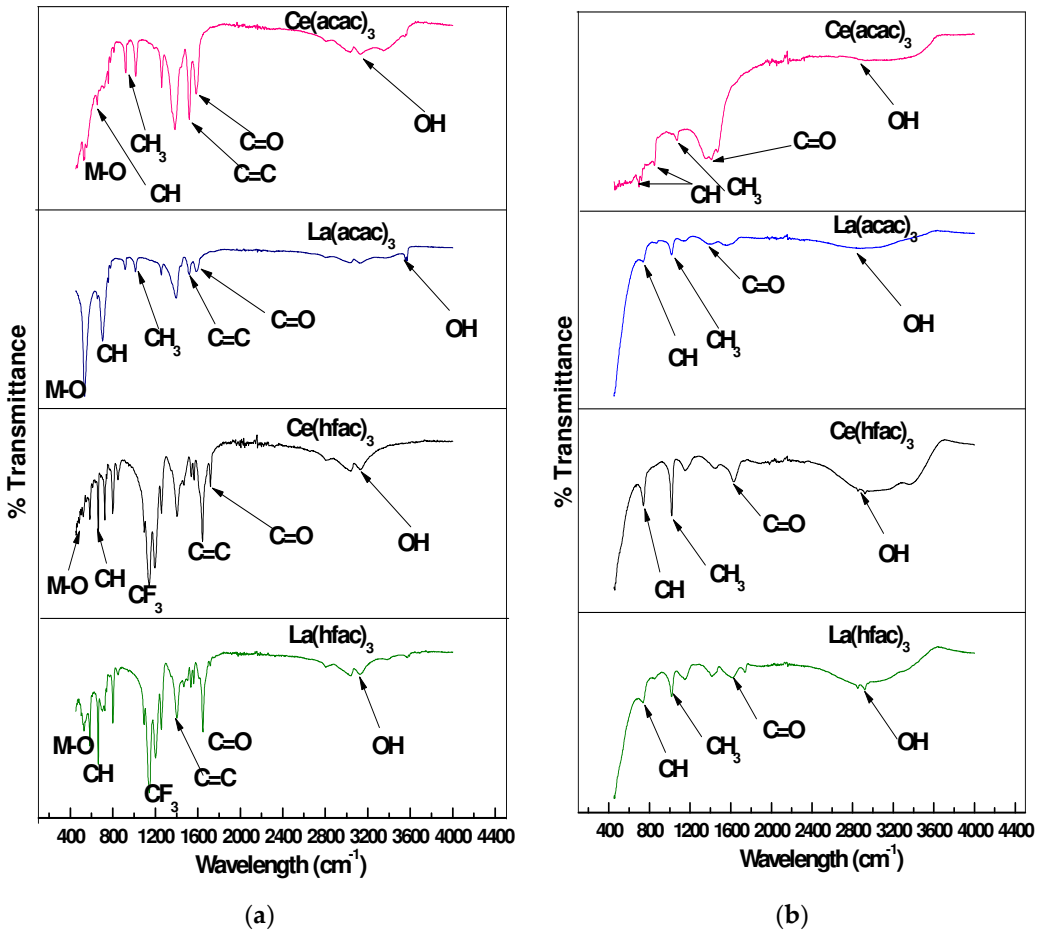

Figure 12. IR spectra of REE(β-diketone)$_3$ inhibitors and the corrosion products formed on mild steel and 304 stainless steel: (**a**) REE β-diketone inhibitor; (**b**) steel REE β-diketone inhibitor film.

4.3.2. Raman Spectroscopy

Raman spectroscopy (RS) was used to map the surface of the mild steel to analyse the nature and mechanism of the adsorption passive film formed on the surface of both mild steel and 304 stainless steel. The spectra were measured in the range of 1900-90 cm^{-1}. It appeared that the obtained frequency bands shifted to a lower wavenumber. This change in the band could be attributed to the coordination between the inhibitor and the steel surface during the film formation. Details of the obtained frequency bands and the spectra obtained in comparison with that of the REE β-diketone complexes are presented in Table 6 and Figure 13. It was observed that the carbonyl C=O stretching and O-H frequency band from the keto-enol group disappeared completely in the steel-REE β-diketone complexes spectrum, indicating the involvement of oxygen present in REE β-diketone complexes in the adsorption process. The shift observed in C-H in-plane, C-H out of plane stretching vibration, and the C=C vibration could be attributed to the interaction of these frequency groups with the steel surface [39,40]. The frequency band observed at 524 cm^{-1} was an indication of metal-oxygen bonds formed as a rare earth oxide (REE–O) protective film on the surface of the steels [13,17,34,41]. The frequency bands in the range (244–250) cm^{-1} and (1306–1311) cm^{-1} could be assigned to stretching vibrations such as for iron oxide (Fe_2O_3), while the frequency band at 377 cm^{-1} was due to lepidocricite (γ-FeOOH), respectively [41–46].

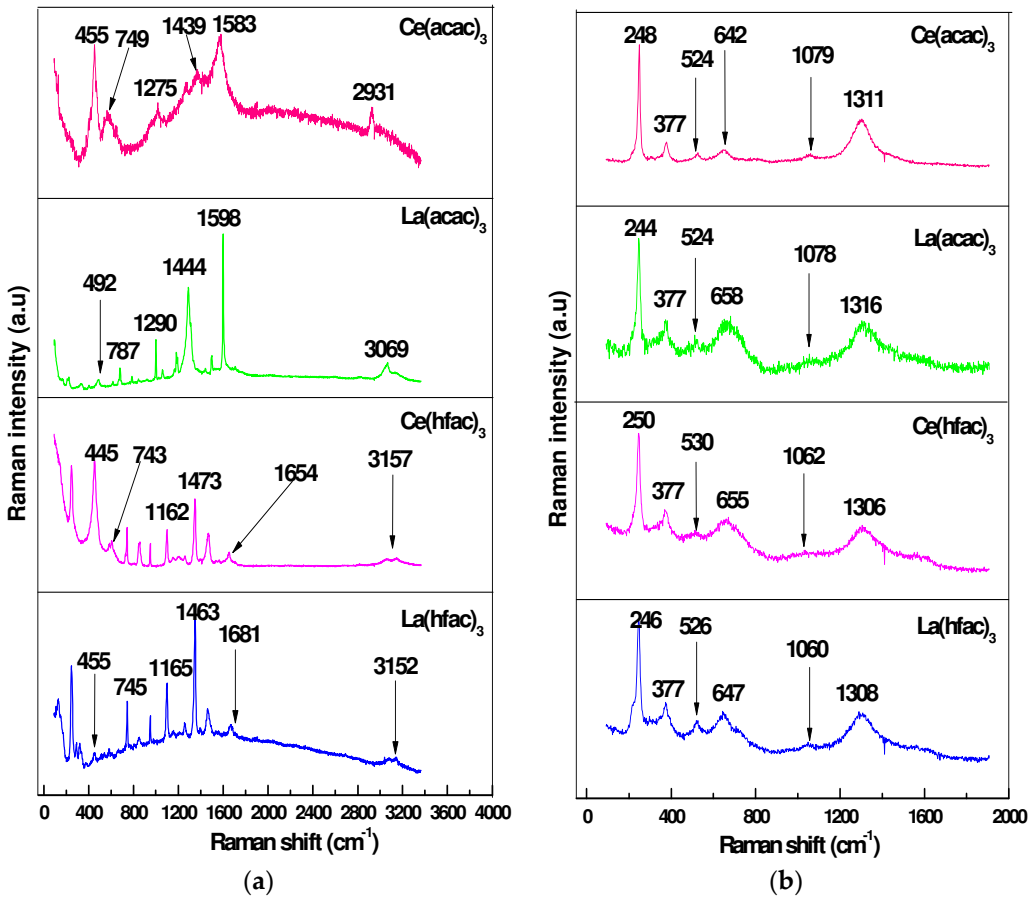

Figure 13. Raman spectra of $Ce(acac)_3$, $La(acac)_3$, $Ce(hfac)_3$, and $La(hfac)_3$ inhibitors and the corrosion products formed on mild steel and 303 SS: (**a**) REE β-diketone inhibitor; (**b**) steel REE β-diketone inhibitor film.

Table 6. Raman frequency band of $Ce(acac)_3$ inhibitor and the corrosion products on mild steel and 304 stainless steel.

Inhibitor Used	Inhibitor Only		Corrosion Product	
	Frequency (cm^{-1})	Assignment	Frequency (cm^{-1})	Assignment
$Ce(acac)_3$	1583	C=O	1311, 248	Fe–O
	455	REE–O	524	REE–O
	2931	O-H	377	γ-FeOOH
$La(acac)_3$	1598	C=O	1316, 244	Fe–O
	492	REE–O	524	REE–O
	3069	O-H	377	γ-FeOOH
$Ce(hfac)_3$	1654	C=O	1306, 250	Fe–O
	445	REE–O	530	REE–O
	3157	O-H	377	γ-FeOOH
$La(hfac)_3$	1681	C=O	1308, 246	Fe–O
	455	REE–O	526	REE–O
	3152	O-H	377	γ-FeOOH

5. Conclusions

- The four tested REE β-diketone inhibitors were found to be reasonably effective corrosion inhibitors against localised corrosion for mild steel and 304 SS in 3.5% NaCl solution and decreased the overall corrosion rates at the concentration of 0.5% in comparison to when the same samples were tested without inhibitors.
- Surface analysis results obtained from Raman spectra confirmed the formation of a protective film layer containing a rare earth element oxide and iron oxide/iron oxyhydroxide on the mild steel and 304 SS. As expected, an increase in temperature did lead to an increase in corrosion rate.
- As the temperature increased, there was a consistent decrease in the value of cathodic Tafel constants compared to when no inhibitors were used under the same conditions and environment. This decrease in the trend of the cathodic Tafel constant confirmed that the tested REE β-diketone complexes acted as cathodic corrosion inhibitors. With the stainless-steel samples exposed to 3.5% NaCl, there was a definitive shift in the corrosion potential to more noble values in the presence of all four corrosion inhibitors, hinting that they act as anodic-type inhibitors. One can, therefore, conclude that the inhibitors are probably mixed corrosion inhibitors whose mode of action depends on the environment and material present when they are used.
- The applied concentration of 0.5% was not sufficient to afford a 100% inhibitor efficiency for either the stainless steel (except at room temperature in the mass loss tests) or the mild steel, especially as the testing temperature increased. It is recommended that a range of higher concentrations be further investigated.
- While one incidence of slight evidence that the type of rare earth element metal present in the corrosion inhibitor could be important was observed, no conclusive evidence could be obtained that either the β-diketone or rare earth element metal played a significant role in the performance of the corrosion inhibitors. Further work with similar inhibitors, in which either or both the β-diketone component or rare earth element in the corrosion inhibitor are varied, should be undertaken in the future.

Author Contributions: Conceptualization, J.H.P.; methodology, O.J.L., J.H.P., D.J.W. and C.B.; validation, O.J.L., J.H.P., D.J.W. and C.B.; formal analysis, O.J.L.; investigation, O.J.L.; resources, J.H.P., D.J.W. and C.B.; data curation, O.J.L.; writing—original draft preparation, O.J.L.; writing—review and editing, O.J.L., J.H.P., D.J.W. and C.B.; supervision, J.H.P., D.J.W. and C.B.; project administration, J.H.P., D.J.W. and C.B. All authors have read and agreed to the published version of the manuscript.

Funding: This research received no external funding.

Data Availability Statement: Data are contained within the article.

Conflicts of Interest: The authors declare no conflict of interest.

References

1. Fouda, A.S.; Abd El-Wahab, S.M.; Attia, M.S.; Youssef, A.O.; Elmoher, H.O. Rare earth metals as eco-friendly corrosion inhibitors for mild steel in produced water. *Der Pharma Chem.* **2015**, *7*, 74–87.
2. Al-Amiery, A.A.; Binti Kassim, F.A.; Kadhum, A.A.H.; Mohamad, A.B. Synthesis and characterization of a novel eco-friendly corrosion inhibition for mild steel in 1 M hydrochloric acid. *Sci. Rep.* **2016**, *6*, 19890. [CrossRef]
3. Pandey, A.; Singh, B.; Verma, C.; Ebenso, E.E. Synthesis, characterization and corrosion inhibition potential of two novel Schiff bases on mild steel in acidic medium. *RSC Adv.* **2017**, *7*, 47148–47163. [CrossRef]
4. Esmailzadeh, S.; Aliofkhazraei, M.; Sarlak, H. Interpretation of Cyclic Potentiodynamic Polarization Test Results for Study of Corrosion Behavior of Metals: A Review. *Prot. Met. Phys. Chem. Surf.* **2018**, *54*, 976–989. [CrossRef]
5. Volarič, B.; Milošev, I. Rare earth chloride and nitrate salts as individual and mixed inhibitors for aluminium alloy 7075-T6 in chloride solution. *Corros. Eng. Sci. Technol.* **2017**, *52*, 201–211. [CrossRef]
6. Gharbi, O.; Thomas, S.; Smith, C.; Birbilis, N. Chromate replacement: What does the future hold? *NPJ Mater. Degrad.* **2018**, *2*, 23–25. [CrossRef]
7. Blin, F.; Leary, S.G.; Wilson, K.; Deacon, G.B.; Junk, P.C.; Forsyth, M. Corrosion mitigation of mild steel by new rare earth cinnamate compounds. *J. Appl. Electrochem.* **2004**, *34*, 591–599. [CrossRef]
8. Somers, A.E.; Hinton, B.R.W.; De Bruin-dickason, C.; Deacon, G.B.; Junk, P.C.; Forsyth, M. New, environmentally friendly, rare earth carboxylate corrosion inhibitors for mild steel. *Corros. Sci.* **2018**, *139*, 430–437. [CrossRef]
9. Fragoza-Mar, L.; Olivares-Xometl, O.; Domínguez-Aguilar, M.A.; Flores, E.A.; Arellanes-Lozada, P.; Jiménez-Cruz, F. Corrosion inhibitor activity of 1,3-diketone malonates for mild steel in aqueous hydrochloric acid solution. *Corros. Sci.* **2012**, *61*, 171–184. [CrossRef]
10. Nam, N.D.; Ha, P.T.N.; Anh, H.T.; Hoai, N.T.; Hien, P.V. Role of hydroxyl group in cerium hydroxycinnamate on corrosion inhibition of mild steel in 0.6 M NaCl solution. *J. Saudi Chem. Soc.* **2019**, *23*, 30–42. [CrossRef]
11. Blin, F.; Leary, S.G.; Deacon, G.B.; Junk, P.C.; Forsyth, M. The nature of the surface film on steel treated with cerium and lanthanum cinnamate based corrosion inhibitors. *Corros. Sci.* **2006**, *48*, 404–419. [CrossRef]
12. Ruiz, M.I.; Heredia, A.; Botella, J.; Odriozola, J.A. Study of the reaction of lanthanum nitrate with metal oxides present in the scale formed at high temperatures on stainless steel. *J. Mater. Sci.* **1995**, *30*, 5146–5150. [CrossRef]
13. Markley, T.A.; Forsyth, M.; Hughes, A.E. Corrosion protection of AA2024-T3 using rare earth diphenyl phosphates. *Electrochim. Acta* **2007**, *52*, 4024–4031. [CrossRef]
14. Nam, N.D.; Thang, V.Q.; Hoai, N.T.; Hien, P. Van Yttrium 3-(4-nitrophenyl)-2-propenoate used as inhibitor against copper alloy corrosion in 0.1 M NaCl solution. *Corros. Sci.* **2016**, *112*, 451–461. [CrossRef]
15. Peng, Y.; Hughes, A.E.; Deacon, G.B.; Junk, P.C.; Hinton, B.R.W.; Forsyth, M.; Mardel, J.I.; Somers, A.E. A study of rare-earth 3-(4-methylbenzoyl)-propanoate compounds as corrosion inhibitors for AS1020 mild steel in NaCl solutions. *Corros. Sci.* **2018**, *145*, 199–211. [CrossRef]
16. Boudellioua, H.; Hamlaoui, Y.; Tifouti, L.; Pedraza, F. Effects of polyethylene glycol (PEG) on the corrosion inhibition of mild steel by cerium nitrate in chloride solution. *Appl. Surf. Sci.* **2019**, *473*, 449–460. [CrossRef]
17. Cotting, F.; Aoki, I.V. Octylsilanol and Ce(III) ions—Alternative corrosion inhibitors for carbon steel in chloride neutral solutions. *J. Mater. Res. Technol.* **2020**, *9*, 8723–8734. [CrossRef]
18. Mohammadi, I.; Shahrabi, T.; Mahdavian, M.; Izadi, M. Cerium/diethyldithiocarbamate complex as a novel corrosion inhibitive pigment for AA2024-T3. *Sci. Rep.* **2020**, *10*, 5043. [CrossRef]
19. Horiguchi, M.; Sawamura, K.; Saito, I.; Hayakawa, Y. β-Diketones as Corrosion Inhibitors for Aluminum in Alkaline Media. *J. Electrochem. Soc. Jpn.* **1968**, *36*, 162–164. [CrossRef]
20. Desa, M.N.; Desai, M.B. Carbonyl compounds as corrosion inhibitors for mild steel in HCl solutions. *Corros. Sci.* **1984**, *24*, 649–660. [CrossRef]
21. Gao, J.; Weng, Y.; Salitanate; Feng, L.; Yue, H. Corrosion inhibition of α,β-unsaturated carbonyl compounds on steel in acid medium. *Pet. Sci.* **2009**, *6*, 201–207. [CrossRef]
22. Avdeev, Y.G.; Kuznetsov, Y.I.; Buryak, A.K. Inhibition of steel corrosion by unsaturated aldehydes in solutions of mineral acids. *Corros. Sci.* **2013**, *69*, 50–60. [CrossRef]
23. Ghanbari, A.; Attar, M.M.; Mahdavian, M. Acetylacetonate complexes as new corrosion inhibitors in phosphoric acid media: Inhibition and synergism study. *Prog. Color Color. Coat.* **2009**, *2*, 115–122.
24. Okawara, T.; Ishihama, K.; Takehara, K. Redetermination of diaquatris(4-oxopent-2-en-2-olato-κ^2O,O')lanthanum(III). *Acta Crystallogr. Sect. E Struct. Rep. Online* **2014**, *70*, m258–m259. [CrossRef] [PubMed]
25. Sastri, V.S.; Ghali, E.; Elboujdaini, M. *Corrosion Prevention and Protection: Practical Solutions*; John Wiley & Sons: Chichester, UK, 2007; ISBN 047002402X.
26. Hinton, B.R. Corrosion Inhibition with Rare Earth Metal Salts. *J. Alloys Compd.* **1992**, *180*, 15–25. [CrossRef]

27. Lin, C.S.; Li, W.J. Corrosion resistance of cerium-conversion coated AZ31 magnesium alloys in cerium nitrate solutions. *Mater. Trans.* **2006**, *47*, 1020–1025. [CrossRef]
28. Forsyth, M.; Seter, M.; Hinton, B.; Deacon, G.; Junk, P. New "Green" corrosion inhibitors based on rare earth compounds. *Aust. J. Chem.* **2011**, *64*, 812–819. [CrossRef]
29. Carneiro, J.; Tedim, J.; Fernandes, S.C.M.; Freire, C.S.R.; Silvestre, A.J.D.; Gandini, A.; Ferreira, M.G.S.; Zheludkevich, M.L. Chitosan-based self-healing protective coatings doped with cerium nitrate for corrosion protection of aluminum alloy 2024. *Prog. Org. Coat.* **2012**, *75*, 8–13. [CrossRef]
30. Matter, E.A.; Kozhukharov, S.; Machkova, M.; Kozhukharov, V. Comparison between the inhibition efficiencies of Ce(III) and Ce(IV) ammonium nitrates against corrosion of AA2024 aluminum alloy in solutions of low chloride concentration. *Corros. Sci.* **2012**, *62*, 22–33. [CrossRef]
31. Gobara, M.; Baraka, A.; Akid, R.; Zorainy, M. Corrosion protection mechanism of Ce4+/organic inhibitor for AA2024 in 3.5% NaCl. *RSC Adv.* **2020**, *10*, 2227–2240. [CrossRef]
32. Forsyth, M.; Wilson, K.; Behrsing, T.; Forsyth, C.; Deacon, G.B.; Phanasgoankar, A. Effectiveness of rare-earth metal compounds as corrosion inhibitors for steel. *Corrosion* **2002**, *58*, 953–960. [CrossRef]
33. Go, L.C.; Depan, D.; Holmes, W.E.; Gallo, A.; Knierim, K.; Bertrand, T.; Hernandez, R. Kinetic and thermodynamic analyses of the corrosion inhibition of synthetic extracellular polymeric substances. *PeerJ Mater. Sci.* **2020**, *2*, e4. [CrossRef]
34. Forsyth, M.; Markley, T.; Ho, D.; Deacon, G.B.; Junk, P.; Hinton, B.; Hughes, A. Inhibition of Corrosion on AA2024-T3 by New Environmentally Friendly Rare Earth Organophosphate Compounds. *Corros. Sci.* **2008**, *64*, 191–197. [CrossRef]
35. Boudellioua, H.; Hamlaoui, Y.; Tifouti, L.; Pedraza, F. Effect of the temperature of cerium nitrate–NaCl solution on corrosion inhibition of mild steel. *Mater. Corros.* **2020**, *71*, 1300–1309. [CrossRef]
36. Yasakau, K.A.; Zheludkevich, M.L.; Lamaka, S.V.; Ferreira, M.G.S. Mechanism of corrosion inhibition of AA2024 by rare-earth compounds. *J. Phys. Chem. B* **2006**, *110*, 5515–5528. [CrossRef] [PubMed]
37. Amadeh, A.; Allahkaram, S.R.; Hosseini, S.R.; Moradi, H.; Abdolhosseini, A. The use of rare earth cations as corrosion inhibitors for carbon steel in aerated NaCl solution. *Anti-Corros. Methods Mater.* **2008**, *55*, 135–143. [CrossRef]
38. Verma, D.K.; Khan, F. Corrosion inhibition of mild steel in hydrochloric acid using extract of glycine max leaves. *Res. Chem. Intermed.* **2016**, *42*, 3489–3506. [CrossRef]
39. Cao, P.; Gu, R.; Tian, Z. Electrochemical and Surface-Enhanced Raman Spectroscopy Studies on Inhibition of Iron Corrosion by Benzotriazole. *Langmuir* **2002**, *18*, 7609–7615. [CrossRef]
40. Caldona, E.B.; Zhang, M.; Liang, G.; Hollis, T.K.; Webster, C.E.; Smith, D.W.; Wipf, D.O. Corrosion inhibition of mild steel in acidic medium by simple azole-based aromatic compounds. *J. Electroanal. Chem.* **2021**, *880*, 114858. [CrossRef]
41. Boudellioua, H.; Hamlaoui, Y.; Tifouti, L.; Pedraza, F. Comparison Between the Inhibition Efficiencies of Two Modification Processes with PEG–Ceria Based Layers Against Corrosion of Mild Steel in Chloride and Sulfate Media. *J. Mater. Eng. Perform.* **2017**, *26*, 4402–4414. [CrossRef]
42. De Faria, D.L.A.; Venâncio Silva, S.; De Oliveira, M.T. Raman microspectroscopy of some iron oxides and oxyhydroxides. *J. Raman Spectrosc.* **1997**, *28*, 873–878. [CrossRef]
43. Jubb, A.M.; Allen, H.C. Vibrational spectroscopic characterization of hematite, maghemite, and magnetite thin films produced by vapor deposition. *ACS Appl. Mater. Interfaces* **2010**, *2*, 2804–2812. [CrossRef]
44. Babouri, L.; Belmokre, K.; Abdelouas, A.; Bardeau, J.F.; El Mendili, Y. The inhibitive effect of cerium carbonate on the corrosion of brass in 3% NaCl solution. *Int. J. Electrochem. Sci.* **2015**, *10*, 7818–7839.
45. Criado, M.; Martínez-Ramirez, S.; Bastidas, J.M. A Raman spectroscopy study of steel corrosion products in activated fly ash mortar containing chlorides. *Constr. Build. Mater.* **2015**, *96*, 383–390. [CrossRef]
46. Lin, B.; Zuo, Y. Corrosion inhibition of carboxylate inhibitors with different alkylene chain lengths on carbon steel in an alkaline solution. *RSC Adv.* **2019**, *9*, 7065–7077. [CrossRef]